INL/CON-15-36957
PREPRINT

Performance Analysis of HF Band FB-MC-SS

IEEE International Conference on Communications (IEEE ICC 2016)

Stephen Andrew Laraway and
Behrouz Farhang-Boroujeny
(University of Utah)

Hussein Moradi
(Idaho National Laboratory)

January 2016

The INL is a
U.S. Department of Energy
National Laboratory
operated by
Battelle Energy Alliance

Performance Analysis of HF Band FB-MC-SS

Stephen Andrew Laraway
Department of Electrical and Computer Engineering
University of Utah
Salt Lake City, Utah
Email: andylaraway@yahoo.com

Hussein Moradi
Wireless Research Team
Idaho National Laboratory
Idaho Falls, Idaho
Email: hussein.moradi@inl.gov

Behrouz Farhang-Boroujeny
Department of Electrical and Computer Engineering
University of Utah
Salt Lake City, Utah
Email: farhang@ece.utah.edu

***Abstract*—In a recent paper the filter bank multicarrier spread spectrum (FB-MC-SS) waveform was proposed as an new method for wideband spread spectrum communications in the HF band. FB-MC-SS is well suited for this application because of its robustness against narrow and partial band interference and because it has good performance over a wide range of delay and Doppler spreads. In this paper we present a study of bit error rate (BER) for this system. In this study channel estimation error and correlation between subcarriers are taken into account. Tailoring the analysis from a different application we give equations for BER that closely match the simulated performance in most situations.**

I. Introduction

The high frequency (HF) skywave propagation channel is a challenging environment for digital communications. In highly disturbed ionospheric conditions the channel has large spreads in both time and frequency. In these conditions channel estimation and equalization are difficult. At the other extreme, in quiet HF conditions a narrow band HF waveform will experience frequency flat fading with fade rates of several seconds. HF waveforms typically include interleaving and forward error correction (FEC) to overcome this fading. Another significant challenge in the HF channel is interference from other users. This interference exists because HF signals propagate long distance making frequency allocation difficult.

Recently FB-MC-SS was introduced for wideband spread spectrum communications in the HF band [1]. Traditionally 3 kHz channels have been used for HF communications. In [1] waveforms with bandwidths ranging from 24 to 200 kHz were proposed. Using signals of this bandwidth offer several advantages over narrow band signals. First, spreading the signal energy over a wide bandwidth results in a more stealthy communication. This is a important characteristic for certain military applications. Second, the wider bandwidth gives increased frequency diversity which results in more robust communications and less latency because interleaving may not be needed.

This manuscript has been authored by Battelle Energy Alliance, LLC under Contract No. DE-AC07-05ID14517 with the U.S. Department of Energy. The United States Government retains and the publisher, by accepting the article for publication, acknowledges that the United States Government retains a nonexclusive, paid-up, irrevocable, world-wide license to publish or reproduce the published form of this manuscript, or allow others to do so, for United States Government purposes. STI Number: INL/CON-15-36957

FB-MC-SS is multicarrier spread spectrum technique that is based on filtered multitone (FMT) [5]. It was initially introduced in [3], [4] and was aimed at terrestrial communications. A significant benefit of this waveform over other spread spectrum modulation techniques is superior performance in partially jammed channels [3], [6]. In addition FB-MC-SS has good performance in time varying multipath channels. In [1] FB-MC-SS was proposed for HF skywave communications. In [1] new algorithms for signal detection were given that are suitable for the harsh HF channel. Simulation results showed that the waveform operated reliably over a wide range of delay and Doppler spreads. In addition, a peak to average power ratio (PAPR) reduction algorithm was introduced in [1] that resulted in PAPRs of 4 to 5 dB.

In [1] bit error rate (BER) simulation results were given. In this paper we provide a theoretical study of these simulated BER results. An analysis of the BER performance is an important tool for designing and verifying a waveform. The simulation results in section VI of [1] show varying amount of implementation loss which depends on the channel conditions. Two of the main causes of this implementation loss are channel estimation error and fading. When the FB-MC-SS signal is detected, estimates of the channel are used to calculated maximum ratio combining (MRC) coefficients. For the system we are considering these channel estimates may have significant error resulting from large Doppler spreads and negative SNR for each subcarrier. The other significant source of implementation loss is fading. To accurately predict the loss from fading, the correlation between the subcarrier channels has to be considered. Assuming that the subcarrier channels are independent will give overly optimist results.

Most paper that analyze the performance of MRC do not consider both channel estimation error and correlation between MRC branches. In the text book analysis of MRC [7] ideal channel estimation and independent and identically (i.i.d) branches are assumed. In [8], [9] channel estimation error is taken into account but i.i.d. branches are assumed. In [10], [11] correlation between subcarriers is considered but not channel estimation error. In [2] the BER performance of a combining algorithm called maximum ratio eigen combining (MREC) is considers for single input multiple output (MISO) systems. This analysis takes into account channel estimation error and branch correlation. The authors also show how this analysis

can be used to analyze the performance of MRC. In this paper we tailer these results to analyze the BER performance of the HF band FB-MC-SS system.

This paper is organized as follows. The FB-MC-SS waveform is described in Section II and the wideband HF channel model is briefly reviewed in Section III. In Section IV some probabilities related to channel estimation error are given. In Section V BER performance is analyzed. Simulation results are presented in Section VI and finally the conclusions are given in Section VII.

Notations: Our presentation is a mix of continuous-time and discrete-time signals. We use $x(t)$ when reference is made to a continuous time signal, and $x[n]$ when referring to a discrete-time signal. Scalars are upper and lower case letters and are not bold. Arrays are bold lower case letters. Matrices are bold upper case letters. The superscripts $(\cdot)^*$, $(\cdot)^{\mathrm{T}}$ and $(\cdot)^{\mathrm{H}}$ represent complex conjugate, transpose and Hermitian transpose, respectively. The notation $\mathbb{E}[\cdot]$ means statistical expectation.

II. FB-MC-SS Waveform

In this section we describe the FB-MC-SS waveform. Throughout this paper perfect frame, carrier and timing synchronization are assumed. Algorithms for synchronization are given in [1]. Also, note that the transmitter and receiver structures described in this section can be implemented efficiently using polyphase techniques [4], [12], [13].

The FB-MC-SS waveform is based on filtered multitone (FMT) (i.e. the subcarrier are non-overlapping) and the symbols are spread over all subcarriers and are not spread over time. A block diagram of the FB-MC-SS transmitter is shown in Fig. 1. In this diagram $s[n]$ are binary phase-shift-keying (BPSK) data symbol with unit magnitude, T is the symbol period and n is discrete time index of the symbols. The symbols are upsampled by L resulting in a sampling period of T/L. The time index m is used for the upsampled data. For each of the N subcarriers the symbols are multiplied by a spreading gain γ_k, filtered by $\mathbf{h}$ and upconverted to frequency f_k. Here $k = 0, 1, ..., N-1$ is the subcarrier index, γ_k are a set of spreading gains with unit magnitude that apply a phase shift to each of the subcarriers, $\mathbf{h}$ is a square-root raised-cosine (SRRC) filter with the roll-off factor $\alpha = 1$ and $\|\mathbf{h}\|^2 = 1$ and f_k are the centers of the subcarrier bands which have $2k/T$ spacing. The subcarriers are summed to form the transmitter output $x[m]$.

A block diagram of the channel model is shown in Fig. 2. In the diagram $\mathbf{c}[m] = \mathbf{c}(mT/L)$ where $\mathbf{c}(t)$ is the time varying impulse response of the channel, $v[m]$ is white Gaussian noise with variance σ_v^2 and $y[m]$ is the channel output. We define $C(f,t)$ to denote the Fourier transform of $\mathbf{c}(t)$. Each subcarrier band is approximated by a flat gain given by $C_k[m] = C(f_k, mT/L)$. Section III describes the HF channel model that specifies $\mathbf{c}(t)$ in more detail.

A block diagram of the receiver is shown in Fig. 3. For each subcarrier the receive signal is down converted, match filtered and decimated to the symbol rate. Since Nyquist filtering is being used and because perfect timing and carrier recovery are assumed, the subcarriers after decimation are given by:

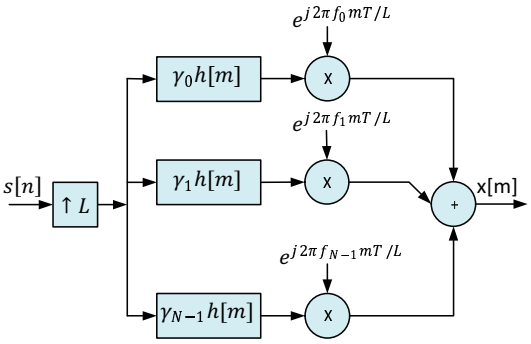

Fig. 1. FB-MC-SS transmitter block diagram.

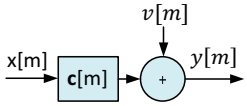

Fig. 2. Channel model.

$$\mathbf{z}_f[n] = s[n]\mathbf{c}_f[n] + \mathbf{v}_f[n] \tag{1}$$

where $\mathbf{z}_f[n] = [z_0[n], z_1[n], \ldots, z_{N-1}[n]]^{\mathrm{T}}$, $\mathbf{c}_f[n] = [C_0[n], C_1[n], \ldots, C_{N-1}[n]]^{\mathrm{T}}$ and $\mathbf{v}_f[n] = [v_0[n], v_1[n], \ldots, v_{N-1}[n]]^{\mathrm{T}}$. The elements of $\mathbf{v}_f[n]$, $v_k[n]$, are independent white Gaussian noise with variance σ_v^2. The f subscript is to indicate that the array is formed from element taken across the subcarriers (i.e. frequency). Finally, each $z_k[n]$ is multiplied by a combining coefficient $w_k^*[n]$ and the subcarriers are summed resulting in an estimate of the transmit symbol, $\hat{s}[n]$. This step may by written as:

$$\hat{s}[n] = \mathbf{w}^{\mathrm{H}}[n]\mathbf{z}_f[n] \tag{2}$$

where $\mathbf{w}[n] = [w_0[n], w_1[n], \ldots, w_{N-1}[n]]^{\mathrm{T}}$.

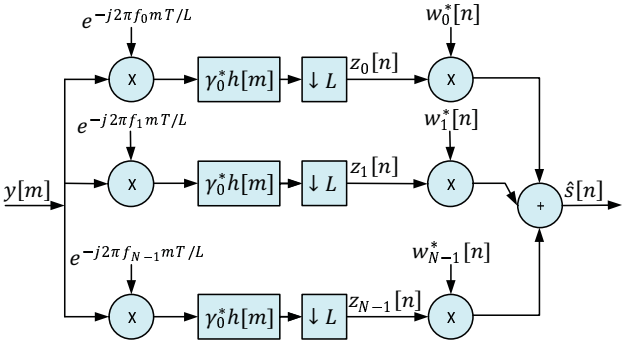

Fig. 3. FB-MC-SS receiver block diagram.

A packet based waveform is considered in this paper. Each packet consists of a preamble section $p[n]$ that is M_{p} BPSK

symbols and a data section that is $M_{\rm d}$ BPSK payload symbols. The preamble section is used to detect the beginning of each packet and perform initial synchronization before detection of the packet.

The channel estimate for each subcarrier, denoted as $\hat{C}_k[n]$, is estimated using a single tap recursive least squares (RLS) filter. Channel estimation is data directed at the beginning of the packet using the pilot and decision directed during the data section of the packet. For this analysis all hard decision are assumed to be correct. In the simulation section we show that in some circumstances decision error can cause additional implementation loss.

The MRC algorithm is used to calculate the combining coefficient. For this analysis the noise variance is assumed to be equal for all subcarriers . Making this assumption, the MRC coefficients are given by:

$$\mathbf{w}[n] = \hat{\mathbf{c}}_f[n-1] \tag{3}$$

where $\hat{\mathbf{c}}_f[n] = [\hat{C}_0[n], \hat{C}_1[n], \ldots, \hat{C}_{N-1}[n]]^{\rm T}$.

III. HF Channel Model

The HF channel is simulated using the wideband HF (WB-HF) channel model described in [14]. The widely used Watterson channel model [15] cannot be used because it is not valid for the wideband signals that are being considered in this paper. A summary of the WB-HF channel model is given in [1]. The WB-HF channel model is a wide-sense stationary uncorrelated scattering (WSSUS) channel model. For each of the ionospheric modes that support propagation, a power delay profile, a delay dependent Doppler shift and a Doppler spectrum specify the channel model. The Doppler spectrum is Gaussian with variance σ_D^2. The channel model parameters are adjusted to simulate specific HF conditions. In this paper a daytime quiet, a nighttime disturbed and a scaled channel are considered. The scattering function of the scaled channel has the same shape as the nighttime disturbed channel but the Dopper spread and delay spread are varied. The scaled channel allows simulating the waveform over a range of delay and Doppler spreads. The daytime and nighttime channel model parameters are summarized in Table I.

TABLE I
Channel Model Parameters

Channel Parameters	Daytime Quiet	Nighttime Disturbed
2σ delay spread	80 μs	615 μs
2σ Doppler spread	0.09 Hz	6.8 Hz
N_{pp}	1	1
A_1	0 dB	0 dB
Δ_1	45 μs	360 μs
α_1	3	3
A_t	-30 dB	-30 dB

For the subsequent performance analysis, the autocorrelation of $C(f,t)$ with respect to time, $\phi_{C_{\Delta t}}(\Delta t)$, and the autocorrelation of $C(f,t)$ with respect to frequency, $\phi_{C_{\Delta f}}(\Delta f)$, are required. The Fourier transform of the power delay profile of the channel impulse response gives $\phi_{C_{\Delta t}}(\Delta t)$ [7]. The channel frequency response, $C(f,t)$, at a given frequency has the same power spectral density as $\mathbf{c}(t)$. Thus, $C(f,t)$ for a constant f has a Gaussian power spectral density with variance σ_D^2. The inverse Fourier transform gives the autocorrelation function, $\phi_{C_{\Delta t}}(\Delta t)$, which is also Gaussian, i.e.,

$$\phi_{C_{\Delta t}}(\Delta t) = \sigma_{C_k}^2 \exp\left(-\frac{\Delta t^2}{2\sigma_\phi^2}\right) \tag{4}$$

where $\sigma_{C_k}^2 = \mathbb{E}[|C_k[n]|^2]$ and $\sigma_\phi^2 = 1/(4\pi^2\sigma_D^2)$.

IV. RLS Channel Estimation Error

In this section we derive several probabilities related to channel estimation error that are required to calculate the bit error probability. Assuming that $s[n] = 1$, the channel estimation algorithm for the k^{th} subcarrier can be modeled as shown in Fig. 4. The block labeled $G(z)$ is the single RLS channel estimation filter. A single tap RLS filter can be approximated as an FIR filter with impulse response:

$$\mathbf{g}(\lambda) = (1-\lambda)[1, \lambda, \lambda^2, \ldots, \lambda^{L-1}]^{\rm T} \tag{5}$$

where λ is the forget factor of the RLS filter and L is the FIR filter length. The filter length is chosen so that λ^L is close to zero. The channel estimate is given by:

$$\hat{C}_k[n-1] = \mathbf{g}^{\rm T}(\lambda)\mathbf{z}_{t,k}[n] \tag{6}$$

where $\mathbf{z}_{t,k}[n] = [z_k[n-1], z_k[n-2], z_k[n-3], \ldots]^{\rm T}$. The t subscript is to indicate that the array is formed from element taken across time. The channel estimation error is given by:

$$e_k[n] = C_k[n] - \hat{C}_k[n-1]. \tag{7}$$

The channel estimation error is calculated using $\hat{C}[n-1]$ because $\hat{s}[n]$ is calculated using $\hat{C}[n-1]$.

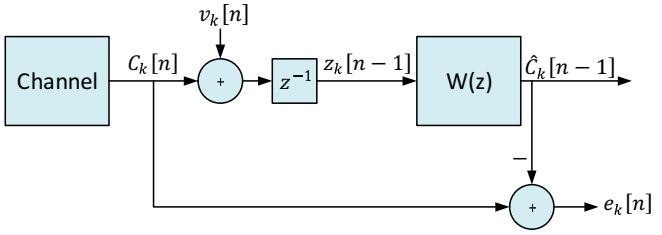

Fig. 4. Channel estimation for the k^{th} subcarrier.

The cross-correlation matrix is defined as

$$\mathbf{p}_k = \mathbb{E}[\mathbf{z}_{t,k}[n]C_k^*[n]] \tag{8}$$

and the autocorrelation matrix is defined as

$$\mathbf{R}_k = \mathbb{E}[\mathbf{z}_{t,k}[n]\mathbf{z}_{t,k}^{\rm H}[n]]. \tag{9}$$

The $i^{\rm th}$ element of $\mathbf{p}_k$ is $p_i = \phi_{C_{\Delta t}}(iT)$ and the $ij^{\rm th}$ element of $\mathbf{R}_k$ is $r_{i,j} = \phi_{C_{\Delta t}}((i-j)T) + \sigma_v^2\delta(i-j)$.

Using 6, 7, 8 and 9 the following expectation can be calculated:

$$\mathbb{E}[|\hat{C}_k[n]|^2] = \sigma_{\hat{C}_k}^2 = \mathbf{g}^{\rm T}\mathbf{R}_k\mathbf{g}, \tag{10}$$

and

$$\mathbb{E}[C_k^*[n]\hat{C}_k[n]] = \sigma_{C_k\hat{C}_k}^2 = \mathbf{g}^{\rm T}\mathbf{p}_k. \tag{11}$$

V. BER Performance Analysis

In [2], [16] a BER performance analysis of a combining algorithm called maximal ratio eigen combining (MREC) is given. In this analysis channel estimation error and correlated subcarrier are accounted for. The focus of this analysis is single input multiple output (SIMO) antenna arrays. In MREC the Karhunen-Loeve Transform (KLT) is performed on the diversity branches and then the outputs of the KLT are combined using the MRC algorithm. In [2] the authors note that their MREC BER analysis can also be used to analyze the BER performance of MRC systems. In the remainder of this section we summarize this BER analysis as it applies to the HF band FB-MC-SS MRC system that we are considering.

To begin, the KLT is applied to (1). The channel correlation matrix across subcarries is defined as

$$\mathbf{R}_{\mathbf{c}_f} = \mathbb{E}[\mathbf{c}_f^{\mathrm{H}}[n]\mathbf{c}_f[n]]. \tag{12}$$

This matrix is Hermitian and nonnegative definitive. It has eigenvalues λ_k where $\lambda_k > \lambda_{i+1}$ for $k = 0, 1, ..., N-1$ and corresponding eigenvectors $\mathbf{e}_k$. This matrix may be decomposed as:

$$\mathbf{R}_{\mathbf{c}_f} = \mathbf{E}_N \mathbf{\Lambda}_N \mathbf{E}_N^{\mathrm{H}}. \tag{13}$$

Here $\mathbf{E}_N = [\mathbf{e}_0, \mathbf{e}_1, \ldots, \mathbf{e}_{N-1}]$ is a unitary matrix and $\mathbf{\Lambda}_N = \mathrm{diag}([\lambda_0, \lambda_1, \ldots, \lambda_{N-1}])$. The variables in (1) are transformed as follows: $\mathbf{z}'_f[n] = \mathbf{E}_N^{\mathrm{H}}\mathbf{z}_f[n]$, $\mathbf{c}'_f[n] = \mathbf{E}_N^{\mathrm{H}}\mathbf{c}_f[n]$ and $\mathbf{v}'_f[n] = \mathbf{E}_N^{\mathrm{H}}\mathbf{v}_f[n]$. The elements of $\mathbf{c}'_f[n]$ are independent with $\mathbb{E}[|C'_k[n]|^2] = \lambda_i$ and the elements of $\mathbf{v}'_f[n]$ are independent with variance σ_v^2. Using (1) these variable may be related as:

$$\mathbf{z}'_f[n] = s[n]\mathbf{c}'_f[n] + \mathbf{v}'_f[n]. \tag{14}$$

The MRC coefficients for (14) are

$$\mathbf{w}'[n] = \hat{\mathbf{c}}'_f[n-1] \tag{15}$$

and the symbol estimate using (14) and (15) is

$$\hat{s}'[n] = \mathbf{w}'^{\mathrm{H}}[n]\mathbf{z}'_f[n] \tag{16}$$

Using (6) the transformed channel estimates are related to the non-tranformed channel estimates as follows:

$$\hat{\mathbf{c}}'_f[n] = \mathbf{Z}'[n]\mathbf{g} = \mathbf{E}_N^{\mathrm{H}}\mathbf{Z}[n]\mathbf{g} = \mathbf{E}_N^{\mathrm{H}}\hat{\mathbf{c}}_f[n] \tag{17}$$

where $\mathbf{Z}[n] = [\mathbf{z}_f[n], \mathbf{z}_f[n-1], \ldots, \mathbf{z}_f[L-1]]$ and $\mathbf{Z}'[n] = [\mathbf{z}'_f[n], \mathbf{z}'_f[n-1], \ldots, \mathbf{z}'_f[L-1]]$. Now the relationship between $\hat{s}[n]$ and $\hat{s}'[n]$ can be found:

$$\hat{s}'[n] = \hat{\mathbf{c}}'^{\mathrm{H}}_f[n-1]\mathbf{z}'_f[n] = \hat{\mathbf{c}}^{\mathrm{H}}_f[n-1]\mathbf{E}_N\mathbf{E}_N^{\mathrm{H}}\mathbf{z}_f[n] = \hat{s}[n] \tag{18}$$

Since the symbol estimates are equal the BER analysis can be performed using the transformed variable.

In [16] equations for BER are derived using the transformed variables. Using the KLT greatly simplifies the analysis becasue the transformed subcarries are independent. The BER is given by [2, equation (39)]:

$$P_e = \frac{1}{2}\sum_{k=1}^{N} S_k(1 - \mu_k\nu_k) \tag{19}$$

where

$$S_k = \prod_{\substack{j=1 \\ j\neq k}}^{N} \frac{1}{a_j^2(s_{j,1} - s_{k,1})(s_{j,2} + s_{k,2})} \tag{20}$$

and where

$$a_k^2 = \frac{1}{4}\sigma_v^2\sigma^2_{\hat{C}'_k}(1 + (1-\mu_k^2)\Gamma_k) \tag{21}$$

and where

$$s_{k,\{1,2\}} = \frac{2\nu_k}{\sqrt{\sigma^2_{\hat{C}'_k}\sigma^2_{C'_k}}}\frac{1}{1 \mp \mu_k\nu_k} \tag{22}$$

and where

$$\Gamma_k = \lambda_k/\sigma_v^2 \tag{23}$$

and where

$$\nu_k = \sqrt{\frac{\Gamma_k}{\Gamma_k + 1}} \tag{24}$$

and where

$$\mu_k = \frac{\sigma^2_{C'_k\hat{C}'_k}}{\sqrt{\sigma^2_{C'_k}\sigma^2_{\hat{C}'_k}}}. \tag{25}$$

Note that $\sigma^2_{C'_k} = \lambda_k$ and that $\sigma^2_{\hat{C}'_k}$ and $\sigma^2_{C'_k\hat{C}'_k}$ can be calculated using (10) and (11), respectively.

VI. Simulation Results

In this section the analytically predicted performance is compared with simulation results. In the preceding analysis perfect synchronization was assumed, frequency flat fading over the subcarrier bandwidth was assumed and decision error were not taken into account. These simplifications were not made in the simulation. The simulations used the algorithms described in [1] for packet detection, timing recovery, channel and noise variance estimation and MRC.

The simulation results are given for the symbol period $T = 4$ ms. This corresponds to a symbol rate $f_s = 1/T = 250$ symbols/second. We examine two choices of N, 48 and 400. The first choice results in a transmission bandwidth of 24 kHz, a value that matches the existing wideband HF waveforms, [17]. The second choice results in a transmission bandwidth of 200 kHz. Since we have fixed T a wider bandwidth results in a larger processing gain and a more robust communication but not a higher data rate. The packet length parameters used in the simulations are $M_{\mathrm{p}} = 96$ and $M_{\mathrm{d}} = 1000$. The simulations do not include forward error correction (FEC) and interleaving. Accounting for the overhead from the preamble, the information bit rate is 228 bits/second.

The BER results are presented as SNR (signal power divided by in-band noise power) varies. SNR is used instead of E_s/N_o to highlight that the receive signal is well below the noise floor. SNR can be converted to E_s/N_o using the conversion $E_s/N_o = 2N \times$ SNR.

BER curves are plotted in Fig. 5 for the daytime quiet channel and in Fig. 6 for the nighttime disturbed channel. The nightime disturbed plot includes simulation results where the receiver had knowledge of the transmit symbols for RLS

adaption (i.e. there were no decision errors). Table II gives the simulated and theoretical SNR required for BER $= 10^{-3}$ over a range of delay spread values and Table III gives these same values over a range of Doppler spread values. For some cases BER $= 10^{-3}$ cannot be reached even at high SNR. These cases are labeled CL, for channel limited. The following observations can be made from these results:

- The daytime quiet channel simulated curves closely match the analysis curves.
- The nightime disturbed simulated curves closey match the analysis curve when the reciever has knowledge of the symbols. When the reciever does not have knowledge of the symbols the simulated performance is worse than the predicted performance. This shows that decision errors are causing implementation loss.
- The 24 kHz waveform BER curve experience flaring from fading. The 200 kHz waveform BER performance does not have this flaring because it has eight time greater frequency diversity.
- The implementation loss from decision errors is greater for higher Doppler spreads. When the Doppler spread is large there is less averaging in the RLS algorithm (the RLS forget factor is small). Thus, decision error to have a greater impact.
- From Table table xx. Analysis does not match simulations when delay spread is large. This is because assumption that subcarriers are flat is not valid. (note: maybe we could do analysis to how much this impact performance.)
- From Table II the analysis and the simulation do not match for large values of delay spread. As the delay spread becomes large the assumption that the subcarriers experience flat fading is not accurate.
- The close match between the simulated results and the analysis shows that the synchronization algorithms given in [1] are working well. There would be additional implementation loss not predicted by the analysis if the synchronization algorithms were causing implementation loss.
- The 200 kHz and 24 kHz waveforms can function reliably at SNR values as low as -19 dB and -10 dB, respectively. This allows operation well below the noise floor, resulting in stealthy communication.
- The superior performance of the 200 kHz waveform over 24 kHz waveform comes from the larger processing gain of the former.

TABLE II
SNR REQUIRED FOR $BER = 10^{-3}$. SCALED NIGHTTIME DISTURBED CHANNEL WITH 2 HZ DOPPLER SPREAD

2σ delay spread (ms)	0.125	0.25	0.5	1	2	4	8
Sim. 24 kHz	CL	-9.8	-10.5	-10.7	-9.9	-7.3	CL
Ana. 24 kHz	-8.7	-10.0	-10.7	-11.1	-11.2	-11.2	-11.2
Sim. 200 kHz	-17.9	-18.0	-18.2	-18.0	-17.1	-14.8	CL
Ana. 200 kHz	-17.8	-18.0	-18.2	-18.2	-18.2	-18.2	-18.2

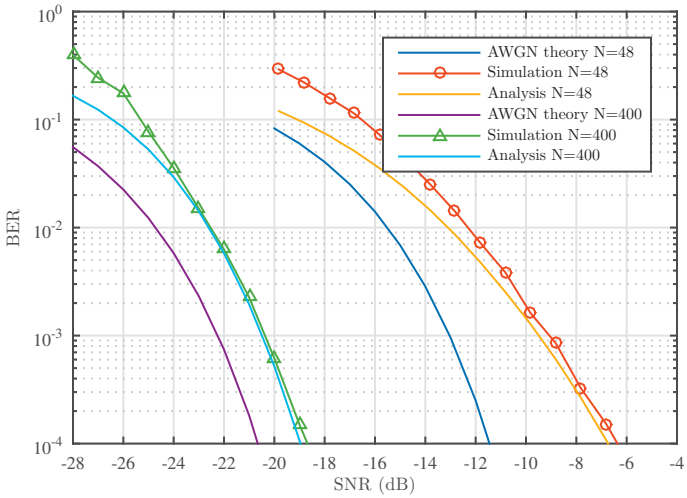

Fig. 5. Daytime quiet channel BER curves (Add footnote about not matching [1]?).

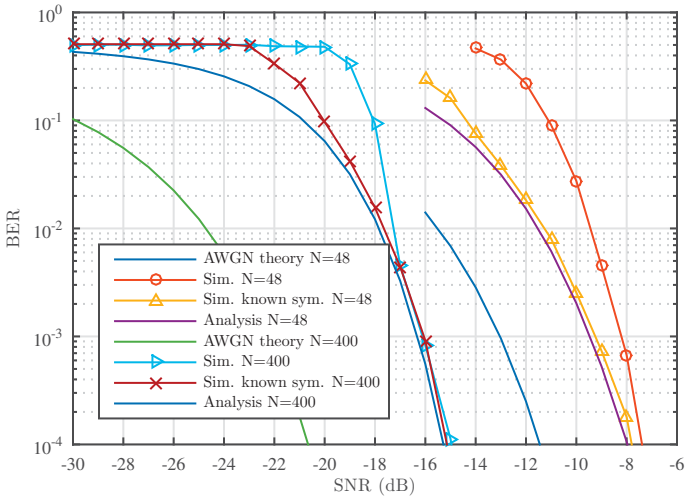

Fig. 6. Nighttime disturbed channel BER curves.

VII. CONCLUSION

In this paper we gave a analystical analysis of the BER performance of the HF FB-MC-SS system describe in [1]. For this analysis we tailor the results of [2] for RLS channel estimation and the wide band frequency channel. For most cases the predicted BER performance is very close to simulated performance. This shows that the synchornization algorithms are working well. When the delay spread or Doppler spead is very large the simlated implementation loss may be higher than predicted by the equations.

REFERENCES

[1] S. Laraway, H. Moradi, and B. Farhang-Boroujeny, "Hf band filter bank multi-carrier spread spectrum," in *IEEE Military Communications Conference (MILCOM)*, 2015.

[2] C. Siriteanu and S. D. Blostein, "Maximal-ratio eigen-combining for smarter antenna arrays," *Wireless Communications, IEEE Transactions on*, vol. 6, no. 3, pp. 917–925, 2007.

TABLE III
SNR REQUIRED FOR $BER = 10^{-3}$. SCALED NIGHTTIME DISTURBED CHANNEL WITH 0.5 MS DELAY SPREAD

2σ delay spread (ms)	0.5	1	2	4	8	16
Sim. 24 kHz	-11.4	-11.2	-10.5	-9.8	-5.5	-4.5
Ana. 24 kHz	-11.6	-11.2	-10.7	-10.0	-9.0	-7.8
Sim. 200 kHz	-19.7	-19.1	-18.2	-17.0	-15.6	-13.4
Ana. 200 kHz	-20.0	-19.2	-18.1	-17.2	-16.0	-14.5

[3] D. L. Wasden, J. Loera, H. Moradi, and B. Farhang-Boroujeny, "Design and implementation of a multicarrier spread spectrum communication system," in *Military Communications Conference, 2012-MILCOM 2012*. IEEE, 2012, pp. 1–7.

[4] D. L. Wasden, H. Moradi, and B. Farhang-Boroujeny, "Design and implementation of an underlay control channel for cognitive radios," *Selected Areas in Communications, IEEE Journal on*, vol. 30, no. 10, pp. 1875–1889, 2012.

[5] G. Cherubini, E. Eleftheriou, and S. Olcer, "Filtered multitone modulation for very high-speed digital subscriber lines," *Selected Areas in Communications, IEEE Journal on*, vol. 20, no. 5, pp. 1016–1028, 2002.

[6] B. Farhang-Boroujeny and C. Furse, "A robust detector for multicarrier spread spectrum transmission over partially jammed channels," *Signal Processing, IEEE Transactions on*, vol. 53, no. 3, pp. 1038–1044, 2005.

[7] A. Goldsmith, *Wireless communications*. Cambridge university press, 2005.

[8] M. J. Gans, "The effect of gaussian error in maximal ratio combiners," *Communication Technology, IEEE Transactions on*, vol. 19, no. 4, pp. 492–500, 1971.

[9] R. Annavajjala and L. B. Milstein, "Performance analysis of linear diversity-combining schemes on rayleigh fading channels with binary signaling and gaussian weighting errors," *Wireless Communications, IEEE Transactions on*, vol. 4, no. 5, pp. 2267–2278, 2005.

[10] J. N. Pierce and S. Stein, "Multiple diversity with nonindependent fading," *Proceedings of the IRE*, vol. 48, no. 1, pp. 89–104, 1960.

[11] S. Siwamogsatham, M. P. Fitz, and J. H. Grimm, "A new view of performance analysis of transmit diversity schemes in correlated rayleigh fading," *Information Theory, IEEE Transactions on*, vol. 48, no. 4, pp. 950–956, 2002.

[12] P. P. Vaidyanathan, *Multirate systems and filter banks*. Pearson Education, 1992.

[13] B. Farhang-Boroujeny, *Signal processing techniques for software radios, 2nd edition*. Lulu publishing house, 2011.

[14] J. F. Mastrangelo, J. J. Lemmon, L. Vogler, J. A. Hoffmeyer, L. E. Pratt, and C. J. Behm, "A new wideband high frequency channel simulation system," *Communications, IEEE Transactions on*, vol. 45, no. 1, pp. 26–34, 1997.

[15] C. Watterson, J. Juroshek, and W. D. Bensema, "Experimental confirmation of an hf channel model," *Communication Technology, IEEE Transactions on*, vol. 18, no. 6, pp. 792–803, 1970.

[16] C. Siriteanu and S. D. Blostein, "Maximal-ratio eigen-combining: a performance analysis," *Electrical and Computer Engineering, Canadian Journal of*, vol. 29, no. 1/2, pp. 15–22, 2004.

[17] *MIL-STD-188-110C Interoperability and Performance Standards for Data Modems*, Std., SEPTEMBER 2011.

[18] B. Farhang-Boroujeny, *Adaptive filters: theory and applications*. John Wiley & Sons, 2013.